Redox Biology 43 (2021) 102002

Contents lists available at ScienceDirect

Redox Biology

journal homepage: www.elsevier.com/locate/redox

Plasmalogen attenuates the development of hepatic steatosis and cognitive deficit through mechanism involving p75NTR inhibition

Yanjun Liu [a,c,1], Peixu Cong [a,1], Tao Zhang [a,d], Rui Wang [a], Xiaoxu Wang [a], Junyi Liu [a], Xinceng Wang [a], Jie Xu [a,**], Yuming Wang [a], Jingfeng Wang [a,***], Changhu Xue [a,b,*]

[a] College of Food Science and Engineering, Ocean University of China, 5 Yushan Road, 266003, Qingdao, Shandong Province, China
[b] Qingdao National Laboratory for Marine Science and Technology, 266235, Qingdao, Shandong Province, China
[c] School of Food Science and Technology, Jiangnan University, 1800, Lihu Road, 214122, Wuxi, Jiangsu Province, China
[d] College of Food Science and Engineering, Nanjing University of Finance and Economics, Nanjing 210023, Jiangsu, China

ARTICLE INFO

Keywords:
Plasmalogen
p75 neurotrophin receptor
Steatosis
Cognitive deficit

ABSTRACT

Emerging evidence suggests that the reduction of ethanolamine plasmalogen (PlsEtn) is associated with in Alzheimer's disease and metabolic diseases. However, the mechanistic bases for PlsEtn on the these diseases are not well understood. Plasmalogens are primarily synthesized in the liver and enriched in brain. To this end, the present study sought to investigate the potential role of PlsEtn on steatohepatitis and memory impairments and its underlying mechanism. Here we show that peroxisome dysfunction and impairment of PlsEtn synthesis pathway occurs in both of hippocampus and liver, resulting in the decrease of PlsEtn level in APP/PS1 mice and HFD-fed mice. shGNPAT induced PlsEtn deficiency in hepatocytes induces p75NTR enhancement leading to decreased lipolysis activity, thereby exacerbating steatosis. Moreover, in the brain, PlsEtn administration appears to not only improve steatosis but also prevent Alzheimer's disease through restoration of TrkA/p75NTR balance. Together, our findings reveal a molecular mechanistic insight into the preventive role of plasmalogen modulation against steatosis and memory impairments via p75NTR inhibition.

1. Introduction

An important common feature of Alzheimer's disease (AD) and metabolic disease is altered lipid metabolism, which alters cell and/or tissue function, inducing a panoply of events related to disease pathogenesis [1]. Plasmalogen are naturally occurring phospholipids characterized by the presence of a vinyl ether bond at the sn-1 position [2]. Among them, growing evidence suggests that a special phospholipid, called ethanolamine plasmalogen (PlsEtn) have a close association with AD [3,4]. PlsEtn level declines in situations of metabolic disease, including obesity, liver disease and Alzheimer's disease [5–7]. Another recent study uncovered a novel link between hepatic free cholesterol accumulation and plasmalogen homeostasis through GNPAT (Glyceronephosphate O-Acyltransferase) regulation [8]. PlsEtn generated in the liver, have been found to play a crucial role in synaptic function in the brain by Kling et al. [9–11]. Scientists have presented an age-related deficiency of plasmalogens lead to an increased risk of AD, and presented research pointing to plasmalogen as one of the potential reason in the onset of Alzheimer's disease. Moreover, lipidomic profiling have identified negative associations between plasmalogens and metabolic disease [12]. However, the mechanistic details of plasmalogens on the AD and metabolic disease processes remains largely unknown. Thus, further detailed mechanistic studies is essential to fully understand the role of plasmalogens in AD and metabolic disease.

Several studies have reported that restoring or enhancing PlsEtn levels through PlsEtn or plasmalogens precursor supplementation prevent/treat metabolic and age-related disorders. For example, evidences showed dietary chicken skin plasmalogens caused the decrease of plasma cholesterol and phospholipids (Pls) in rats [13], while administration of plasmalogens attenuated neuroinflammation in mice [14]. Our previous study show dietary eicosapentaenoic acid enriched ethanolamine plasmalogen (PlsEtn) alleviated atherosclerosis via reducing

* Corresponding author. College of Food Science and Engineering, Ocean University of China, 5 Yushan Road, 266003, Qingdao, Shandong Province, China.
** Corresponding author.
*** Corresponding author.
E-mail addresses: xujie9@ouc.edu.cn (J. Xu), jfwang@ouc.edu.cn (J. Wang), xuech@ouc.edu.cn (C. Xue).
[1] These authors contributed equally to this work.

https://doi.org/10.1016/j.redox.2021.102002
Received 26 March 2021; Received in revised form 2 May 2021; Accepted 4 May 2021
Available online 7 May 2021

total cholesterol levels [15]. Plasmalogen administration was also reported to abolish amyloid-beta (Aβ) protein expression in mice [16]. Furthermore, PlsEtn from chicken skin prevented neuronal cell death in neuronal cells [17,18]. Docosahexaenoic acid enriched ethanolamine plasmalogen (DHA-PlsEtn) strongly reduced γ-secretase activity and reduced Aβ production in SH-SY5Y cells [19]. Of note, 6 months of scallops plasmalogen treatment shown a significant memory improvement among patients with mild AD [20]. Thus, more in-depth mechanisms studies are required to explore further in order to gain a better understanding of PlsEtn function.

p75 neurotrophin receptor (p75NTR), the low-affinity neurotrophins receptor, has been well documented that p75NTR plays a critical role in production of Aβ, neuronal death, neurite degeneration, tau hyperphosphorylation [21–24]. Besides, target p75NTR appears to controls energy expenditure and provide a potential therapeutic intervention for preventing liver steatosis and other metabolic disease [25]. Notably, peroxisome deficiency causes altered neuronal morphology and dysregulation brain-derived neurotrophic factor signaling pathway (one of the ligands for p75NTR) [26]. Since the peroxisome serves as a platform for plasmalogen biogenesis, we hypothesized might p75NTR is involved in the role of PlsEtn in AD and liver diseases. To this end, our studies sought to investigate the potential role of PlsEtn on steatohepatitis and memory impairments and its underlying mechanism, and show that p75NTR inhibition is Involved.

2. Materials and methods

2.1. Animal experiments

All applicable institutional and/or national guidelines for the care and use of animals were followed. All experimental protocols were carried out in accordance with the ARRIVE Guide for the Care and Use of Laboratory Animals [27], and approved by the Animal Ethics Committee of the College of Food Science and Engineering of the Ocean University of China. 20-weeks-old male APP/PS1 and littermate WT mice were purchased from the Model Animal Research Center of Nanjing University, China. PlsEtn was extracted from *C. frondosa* according to our previous method [28]. The APP/PS1 mice were randomly allocated to two groups: APP/PS1 group (APP/PS1, n = 5); APP/PS1 supplemented with 0.1% PlsEtn (PlsEtn, n = 5). After 16 weeks of daily treatment, behavioral tests (Morris water maze test and radial 8-arm maze test) were carried out. All of the mice were housed under a 12-h light/dark cycle at 23 °C and provided with respective diet and water *ad libitum*.

To developed a mice model of obesity, mouse cohorts (C57BL/6J mice, 6-weeks-old) received chow diet (n = 5) and 60 kcal% saturated HFD (Research Diets, D12492, n = 5) for 12 weeks, respectively. C57BL/6J mice, 6-weeks-old, were established to steatosis model by feeding mice a chow diet or high-fat high-sucrose diet (HFSD, Research Diets, D12331), which consisted of 20% protein, 25% fat, and 20% carbohydrate. The HFSD-fed animals were randomly allocated to two groups: HFSD group (HFSD, n = 5); HFSD supplemented with 0.1% PlsEtn (PlsEtn, n = 5). Mice were managed 12 weeks with the respective diet and water *ad libitum*. Another cohort of C57BL/6J mice, 6-weeks-old, were established to insulin resistant model by feeding mice a high-fat high-sucrose diet and received AAV-shGNPAT virus for 6 weeks.

2.2. Plasmids construction

For AAV-mediated genetic manipulations, we generated pAAV2/8 constructs by cloning a cDNA or shRNA expression cassette into the plasmid backbone. The shRNA sequences used were listed as follow: Mouse shGnpat: CTCAATCGGAACACGTATAAC, Mouse p75NTR: GGAGACATGTTCCACAGGCA. AAV gene delivery vectors for shRNA (AAV-shRNA-ctrl, RRID: Addgene_85741) was a gift from Hongjun Song (Addgene plasmid #85741; http://n2t.net/addgene:85741).

2.3. Preparation of recombinant AAV virus

All pAAV vectors were produced in HEK293 cells by the helper virus-free, two-plasmid-based production method. Briefly, subconfluent cells were co-transfected by the PEI method with equimolar amounts of a rep/cap/helper plasmid (pDP8. ape) and a vector plasmid. After 72 h post-transfection, cells were lysed and then treated with benzonase, and further purified by CsCl density gradient centrifugation. Fractions from the gradient were collected, peak fractions were pooled, dialyzed against 1× DPBS containing 10% glycerol, concentrated (Amicon Ultra-15, Millipore, Schwalbach, Germany), filter-sterilized and stored at −80 °C.

2.4. Cell culture

AML12 cells (ATCC Cat# CRL-2254, RRID:CVCL_0140), purchased from American Type Culture Collection (USA), were cultured in DMEM supplemented with 10% FBS and 10 μg ml^{-1} insulin, 5.5 μg ml^{-1} transferrin, 5 ng ml^{-1} selenium, 40 ng ml^{-1} dexamethasone (Sigma) at 37 °C. Palmitic acid (PA, Sigma) were diluted in DMEM containing 2% (w/v) fatty acid-free bovine serum albumin to yield a 400 μM solution of PA complexed to BSA. AML12 cells were treated with palmitic acid/BSA mixture for 48 h. AML12 cells were incubated with PlsEtn (200 μg ml^{-1}) for 24 h. For silent RNA assay to knockdown of GNPAT or p75NTR, lipofectamine 2000 was used for shRNA transfection.

2.5. Lipids analysis by RPLC-MS/MS

All lipid analysis was performed by RPLC-Q Exactive-MS/MS system (Thermo Fisher, Waltham, MA, USA). An Acquity UPLC BEH C18 column (2.1 mm × 100 mm, 1.7 μm) (Waters, MA, USA) was applied. Mobile phase A consisted of acetonitrile/water (60:40, v/v) with 5 mmol ammonium formate and 0.2% ammonia; mobile phase B was isopropanol/acetonitrile (90:10, v/v). The elution gradient was set as follows: 25% B for 2 min; 25%–50% B for 6 min; 50%–90% B for 5 min; 90%–99% B for 6 min and keeping condition (99% B) for 6 min; 99%–25% B for 1 min and keep condition (25% B) for 5 min. The flow rate was set at 0.35 ml min^{-1}; the column oven was maintained at 45 °C. An aliquot of 5 μL was injected into the RPLC-Q Exactive-MS/MS system. The MS operation were set as two steps as follows: 1) Full Scan-ddMS2 positive-ion mode was applied with HESI source; source temperature of 300 °C; Ion transfer tube temperature of 3.5 kV; Sheath gas flow of 38 arbitrary units; Auxiliary gas flow of 10 arbitrary units; a range of *m/z* 200–1000 for MS scans with a resolution of 35000, and a range of *m/z* 100–700 for MS/MS scans with a resolution of 17500. 2) The original Full-scan ddMS2 data were imported into Lipidsearch software for the identification of lipid species and molecular species. After the output of the results, the *m/z* information was manually extracted and compared with the lipid molecular library for accurate qualitative analysis. A list of information including the retention time and precursor ion *m/z* was generated, and imported the PRM model acquisition method. The PRM mode parameters was set as positive-ion mode; isolation window of ion of 1.4 *m/z*; resolution of 17500; the scan worked according to the Inclusion list. The original data collected by PRM mode was imported into Tracefinder 4.1 for peak area extraction and quantitative processing through the established compound database.

2.6. qRT-PCR

Total RNA was extracted from tissues and cells using TRIzol reagent. RNA was reverse transcribed using cDNA Synthesis SuperMix. Real-time PCR was carried out in a quantitative real-time PCR thermocycler with SYBR Green PCR master mix (Roche, Basel, Switzerland) and gene-specific primers. The $2^{-\Delta\Delta CT}$ method was used to analyze the relative changes in gene expression normalized against 36B4 mRNA expression.

2.7. Morris water maze test

A circular pool was filled with water made opaque by milk addition and divided into four quadrants. A black escape platform was located in the center of one quadrant and the mice were subjected to acquisition trial a day for 5 days. The mice were manually guided to the platform, when the mice were failed to locate the platform within 60 s. At last day, the mice were allowed to swim in the pool for 60 s and the number crossing over the previous position of the platform and the time spent in the target quadrant were recorded.

2.8. Immunohistochemistry staining

Mice were euthanized and systemically perfused with phosphate-buffered saline (PBS) and 4% paraformaldehyde solution, then the brain samples were collected and fixed in 4% paraformaldehyde solution for 24–48 h at 4 °C. The samples were then incubated in 30% sucrose for 12 h and embedded in paraffin. The sections were incubated with the primary antibody against anti-Aβ (Abcam, Cat# A85418, RRID:AB_2748979), anti-Iba1 (Servicebio, GB11105), anti-GFAP (Servicebio, GB11096), anti-CD68 (Abcam, Cat# ab125212, RRID:AB_10975465), anti-Tau antibody (Abcam Cat# ab32057, RRID:AB_778254), anti-NGF (Servicebio, GB111206). For histomorphometric analysis, a Leica DM 5000B microscope (Sony, Japan) were used.

2.9. Western blotting

The total protein were extracted and were separated by SDS-PAGE, transferred to PVDF membranes, and incubated with primary antibodies. The following antibodies were used: Anti-HSL (Cell Signaling Technology, Cat# 4107, RRID:AB_2296900), anti-HSL (phospho S563) (Cell Signaling Technology, 4139), anti-ATGL (Cell Signaling Technology Cat# 2439, RRID:AB_2167953), anti-JNK (Cell Signaling Technology, Cat# 9252, RRID:AB_2250373), anti-JNK (Phospho Thr183/Tyr185) (Cell Signaling Technology, Cat# 9251, RRID:AB_331659), Anti-Tau (phospho S396) (Abcam, ab109390), Anti-Tau antibody (Abcam, Cat# ab32057, RRID:AB_778254), anti-Aβ (Abcam, Cat# A85418, RRID:AB_2748979), anti-GFAP (Servicebio, GB11096), Anti-ADAM10 (Abcam, Cat# ab124695, RRID:AB_10972023), Anti-BACE1 (Abcam, Cat# ab108394, RRID:AB_10861218), Anti-Nicastrin (Abcam, Cat# ab3444, RRID:AB_303806), Anti-β-actin antibody (Abcam, Cat# GTX26276, RRID:AB_367161), Anti-IL1β antibody (Abcam, Cat# ab9722, RRID:AB_308765), Anti-TNFα (Abcam, Cat# ab6671, RRID:AB_305641), anti-GSK3β (Abcam, Cat# ab32391, RRID:AB_2115066), anti-GSK3β (phospho Y216+Y279) (Abcam, Cat# ab68476, RRID:AB_10013745), anti-TrkA (Abcam, Cat# ab86474, RRID:AB_1951357), anti-TrkB (Servicebio, GB11295-1), anti-TrkB (phosphp Try816) (Millipore, Cat# ABN1381, RRID:AB_2721199), Anti-Caspase 3 (Cell Signaling Technology, Cat# 9662, RRID:AB_331439), anti-cleaved caspase 3 (Cell Signaling Technology, Cat# 9664, RRID:AB_2070042), anti-Cd11b (Cell Signaling Technology, Cat# 49420, RRID:AB_2799357), anti-TrkA (phosphp Try490) (Cell Signaling Technology Cat# 9141, RRID:AB_2298805), anti-p75NTR (Sangon Biotech, D261027), anti-Bax (Abcam, Cat# ab32503, RRID:AB_725631).

2.10. Determination of Aβ levels

Hippocampus was homogenized in lysis buffer containing a cocktail of protease inhibitors. Each sample was sonicated in 70% formic acid and neutralized with 0.5 M Tris after centrifugation at 10,000 g for 15 min at 4 °C. Soluble and insoluble Aβ were measured using a human amyloid ELISA kit.

2.11. Golgi staining

Brain sections were placed to Golgi dye solution for 3 days, and then transferred to 1% silver nitrate solution for another 3 days.

2.12. Silver staining

NFTs were detected by Bielschowsky silver staining method. Briefly, Brain sections were placed in 10% silver nitrate solution for 15 min and then placed in ammonium silver nitrate solution at 40 °C for 30 min. Sections were placed in 1% ammonium hydroxide solution to stop the reaction.

2.13. Oil red O staining

For Oil Red O staining, the cells and tissue section were fixed with 10% formaldehyde and stained with oil red O solution.

2.14. H&E staining

Mice were euthanized and the tissues were immediately removed and immersed in pre-cooled PBS, fixed in 10% formalin solution for 24–48 h at 4 °C. The samples were then incubated in 70% ethanol for 12 h and embedded in paraffin and sectioned into 5-μm-thick sections. All sections were stained with hematoxylin and eosin.

2.15. Statistical analysis

All values are presented as the means ± SEM where noted. All experiments were repeated at least three times unless stated in the figure legends. Prism 8.0 software (RRID: SCR_002798) was used for statistical analysis and graphical presentation. Our studies comply with the recommendations of the *British Journal of Pharmacology* on experimental analysis [29]. Statistical significance was determined by Student's *t*-test. Probability of p value < 0.05 was indicated a significant difference.

3. Results

3.1. Impaired PlsEtn synthesis in AD mice and HFD-fed mice

PlsEtn is highly abundant in the brain, while its synthesis in the brain is initiated in peroxisomes and completed in the endoplasmic reticulum (Fig. 1A), and the liver is also the primary organ involved in plasmalogen supply [8]. In initial studies, we assessed PlsEtn levels in hippocampus of APP/PS1 mice and found that levels of several PlsEtn were reduced in hippocampus (Fig. 1B) compared with WT (wild type) mice. Among them, *Gnpat*, *Far1*, *Apgs* and Pex7 are genes encoding the enzymes essential for the synthesis of plasmalogens. The mRNA expression levels of *Gnpat*, *Far1* and *Apgs* decreased significantly in hippocampus, whereas *Gnpat* and *Apgs* mRNA expression levels were also significantly reduced in liver of APP/PS1 mice (Fig. 1C and D), compared with WT mice, which confirmed the impairment of PlsEtn synthesis in both of hippocampus and liver of APP/PS1 mice. Moreover, peroxisome homeostasis plays a pivotal role in the biosynthesis of plasmalogen. We found decreased mRNA levels of *Pmp70*, *Pex14*, and *Pex16* (Fig. 1C and D) in the hippocampus and liver of APP/PS1 mice, which suggest peroxisome dysfunction occurs in AD. Similar results as found in the AD mice were also obtained in HFD-fed mice, showing that high fat diet treatment induced the reduction of PlsEtn levels and decreased *Gnpat* expression (Fig. 1E–H) in both of hippocampus and liver. Quantitative real-time PCR (qPCR) analysis showed a dysregulated signaling of peroxisome homeostasis in response to HFD, as indicated by a reduction of *Pmp70* and *Acox* mRNA expression (Fig. 1G and H) in hippocampus and liver of HFD-fed mice. Above data indicated that changes/damages in peroxisome and impaired PlsEtn synthesis in both of APP/PS1 and HFD-fed mice could be involved in the reduction of plasmalogen levels, which appear to be associated with both Alzheimer's disease and high-fat diet (HFD)-induced hepatic steatosis.

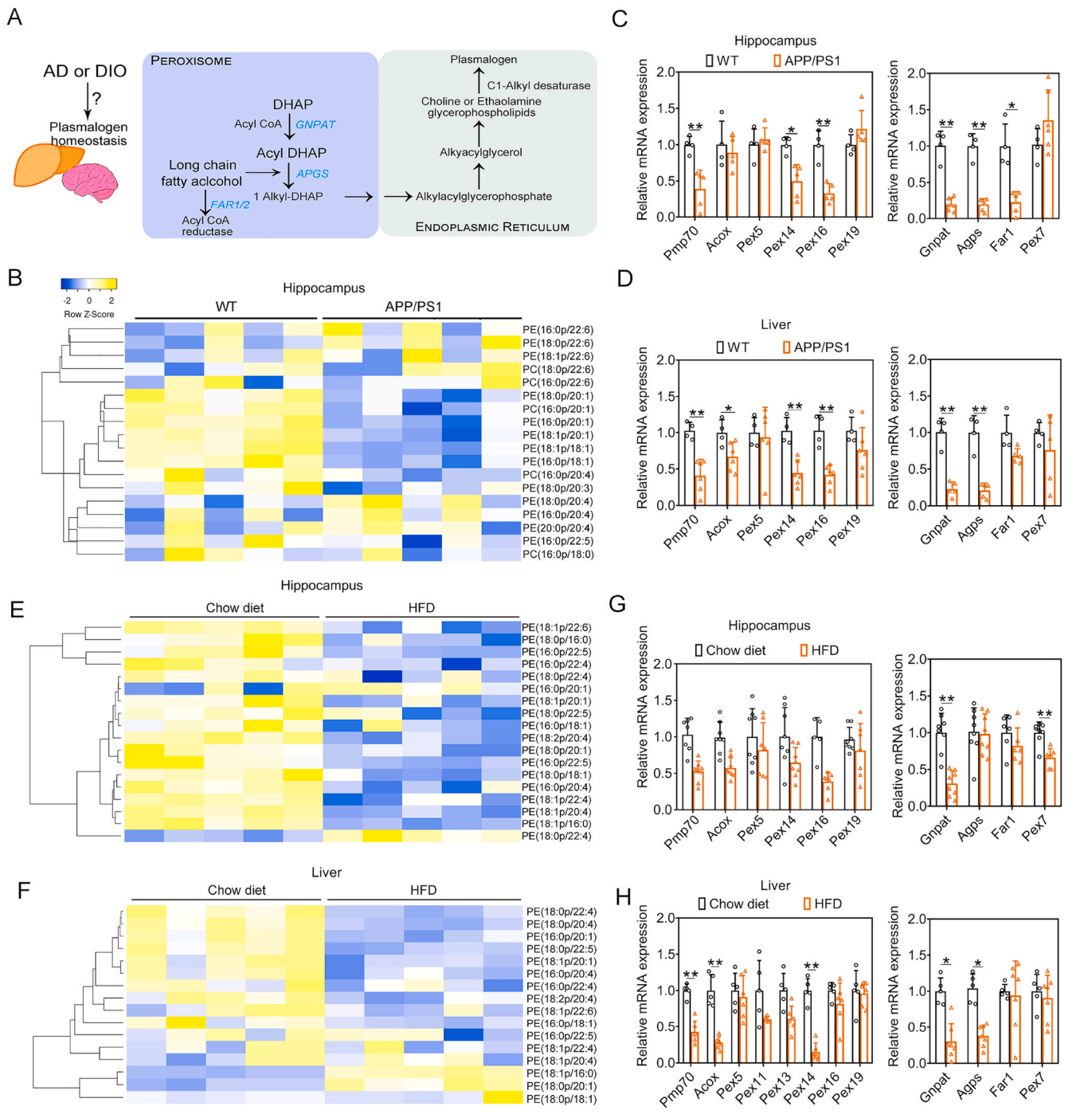

Fig. 1. PlsEtn synthesis was impaired in APP/PS1 and HFD-fed mice. (A) Biosynthetic and catabolic pathways of plasmalogens. (B) Heatmaps illustrate the fold change in individual plasmalogen species in the hippocampus of APP/PS1 mice compared against WT mice. (C and D) Relative mRNA expressions related to peroxisomes homeostasis and PlsEtn synthesis pathway in the hippocampus and liver of APP/PS1 mice compared against WT mice. (E) Heatmaps illustrate the fold change in individual plasmalogen species in the hippocampus of HFSD-fed mice compared against chow diet-fed mice. (F) Heatmaps illustrate the fold change in individual plasmalogen species in the liver of HFSD-fed mice compared against chow diet-fed mice. (G and H) Relative mRNA expressions related to peroxisomes homeostasis and PlsEtn synthesis pathway in the hippocampus and liver of HFSD-fed mice compared against chow diet-fed mice. Statistical significance was determined by Student's *t*-test, *p < 0.05, **p < 0.01 vs WT or Chow diet-fed mice.

3.2. *PlsEtn deficiency aggravates hepatic steatosis via p75NTR inhibition*

The AML12 cell model treated with PA or ethanol (EtOH) was qualified as an in vitro hepatic steatosis model for further silent RNA assay to knockdown of GNPAT to investigate the role of PlsEtn on steatosis. Compared with control group, GNPAT shRNA treatment increased the quantity of lipid droplets (LDs) as indicated by Oil Red O staining in EtOH (Suppl. Fig. 1) or PA (Fig. 2A) induced AML12 steatosis models, which suggest PlsEtn deficiency appears to induce hepatic steatosis. Of note, shGNPAT induced PlsEtn deficiency resulted in increased p75NTR and elevated levels of *p*-JNK in PA-treated AML12 cells (Fig. 2B). Meanwhile, to evaluate its underlying mechanism of PlsEtn deficiency on hepatic steatosis, we measured the p75NTR expression in the liver and hippocampus from HFD-fed mice and APP/

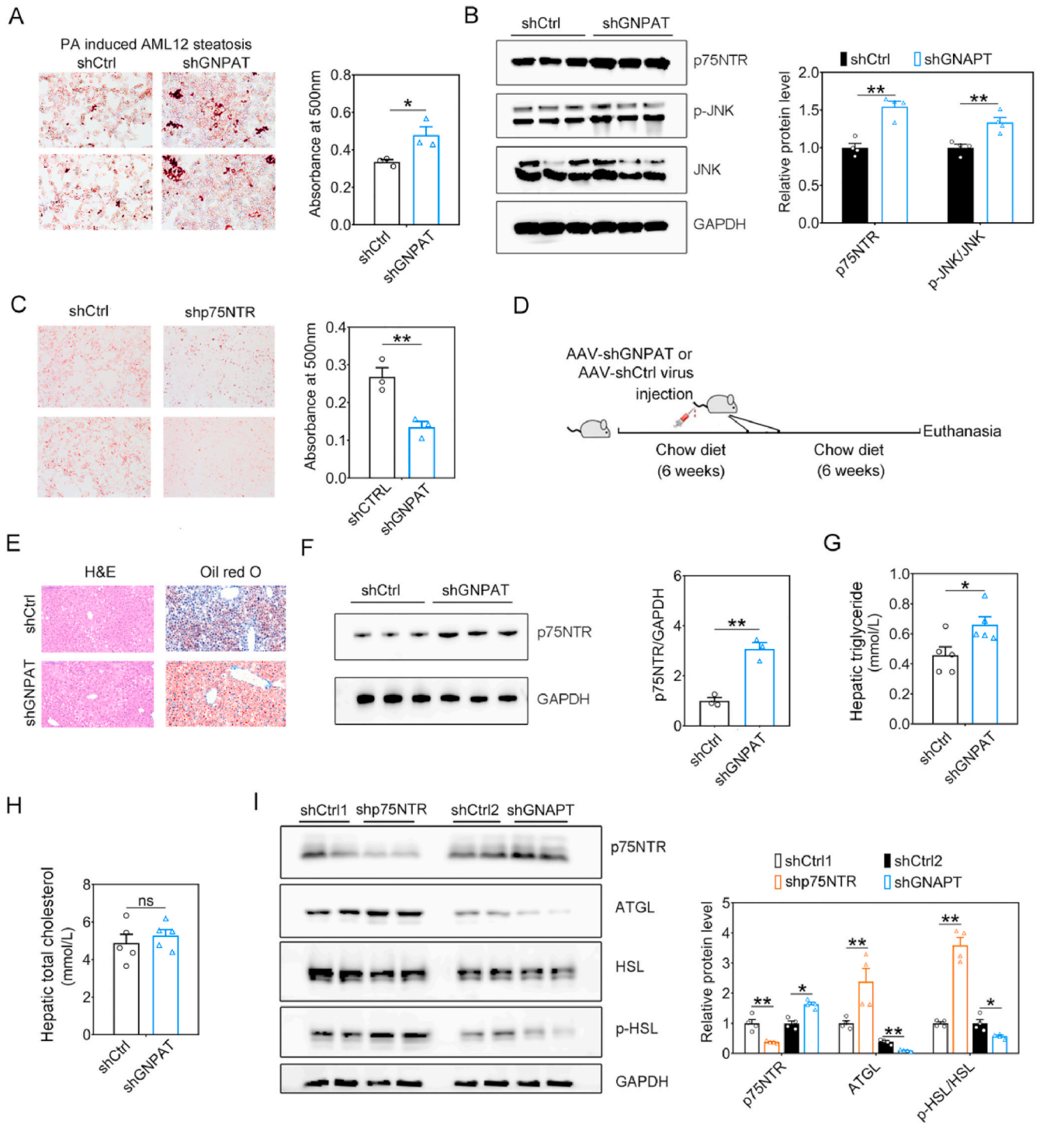

Fig. 2. PlsEtn deficiency aggravates hepatic steatosis via p75NTR. (A) AML12 cells were transfected with shGNPAT or scrambled control (shCTRL1) and subsequently exposed to 400 μM PA for an additional 48 h. Lipid droplets accumulation within the AML12 cells were determined by Oil-red O staining and quantified at 500 nm. (B) Representative Western blot indicating the protein expression of p75NTR and lipolysis related genes in AML12 cells treated with shGNPAT. (C) AML12 cells were transfected with shp75NTR or scrambled control (shCTRL2) and subsequently exposed to 400 μM PA for an additional 48 h. Lipid droplets accumulation were determined by Oil-red O staining and quantified at 500 nm. (D) 6-week old mice was used to develop hepatic steatosis under high fat high fructose diet and treated with recombinant AAV virus of shGnpat. (E) Photomicrographs depicting the liver from AAV-shGnpat-treated and HFSD-fed mice (n = 5 mice/group) stained for H&E and Oil red O. (F) Representative Western blot indicating the protein expression of p75NTR and lipolysis related genes in AAV-shGnpat-treated and HFSD-fed mice. (G) Hepatic triglyceride levels in AAV-shGnpat-treated and HFSD-fed mice. (H) Hepatic total cholesterol in AAV-shGnpat-treated and HFSD-fed mice. (I) Representative Western blot indicating the protein expression of p75NTR and lipolysis related genes in AML12 cells treated with shp75NTR. Statistical significance was determined by Student's *t*-test, *$p < 0.05$, **$p < 0.01$ vs scrambled control. (For interpretation of the references to colour in this figure legend, the reader is referred to the Web version of this article.)

PS1 mice. Long-term HFD treatment for 12 weeks resulted in up-regulated p75NTR in both of liver and hippocampus, whereas both of liver and hippocampus also exhibited increased p75NTR expression in APP/PS1 mice (Suppl. Fig. 2A–D). Study has identified p75NTR knockout could prevent HFD-induced obesity [25]. Consistent with the result in p75NTR knockout mice, p75NTR shRNA (shp75NTR) treatment reduced the quantity of lipid droplets (Fig. 2C) in PA-treated AML12 cells. To elucidate the influence of PlsEtn deficiency (GNPAT knock-down) on hepatic steatosis, 6-week old mice was used to develop hepatic steatosis under high fat high fructose diet and treated with recombinant AAV virus of shGnpat (Fig. 2D). After 6 weeks, shGnpat-treated mice exhibited increased lipid accumulation, higher TG levels as well as higher expression of p75NTR (Fig. 2E–H) in liver tissue than shCtrl virus treatment. In PA-treated AML12 cells, p75NTR shRNA (shp75NTR) treatment induced lipolysis (Fig. I) as indicated by increased expression of adipose triglyceride lipase (ATGL) and phosphalytion of hormone-sensitive lipase (HSL), while shGNPAT induced PlsEtn deficiency resulted in enhanced p75NTR expression and reduced lipolysis, which suggest that shGnpat induced PlsEtn deficiency exacerbated hepatic steatosis via the alteration of p75NTR mediated lipolysis (Fig. 2I).

3.3. Dietary PlsEtn improve hepatic steatosis via p75NTR inhibition

To explore whether hepatic steatosis was improved by PlsEtn and elucidate the influence of PlsEtn administration on hepatic steatosis, we treated PA-treated AML12 cells with PlsEtn from sea cucumber. Indeed, co-treatment with PlsEtn reduced the quantity and size of LDs as indicated by Oil Red O staining (Fig. 2A–B), which indicated that PlsEtn administration improve hepatic lipid accumulation in PA-treated AML12 cells. Intriguingly, APP/PS1 mice exhibited hepatic steatosis and lipid accumulation in brain (Suppl. Fig. 3A–B). We further determine the role of PlsEtn administration in hepatic steatosis and lipid accumulation of APP/PS1 mice and HFSD (high-fat, high-sugar diet) induced hepatic steatosis mice model, and we hypothesized that PlsEtn might contribute to improve aberrant hepatic lipid accumulation in APP/PS1 mice and HFSD-fed mice. As expected, PlsEtn treatment led to improved lipid accumulation in both of hippocampus and liver section

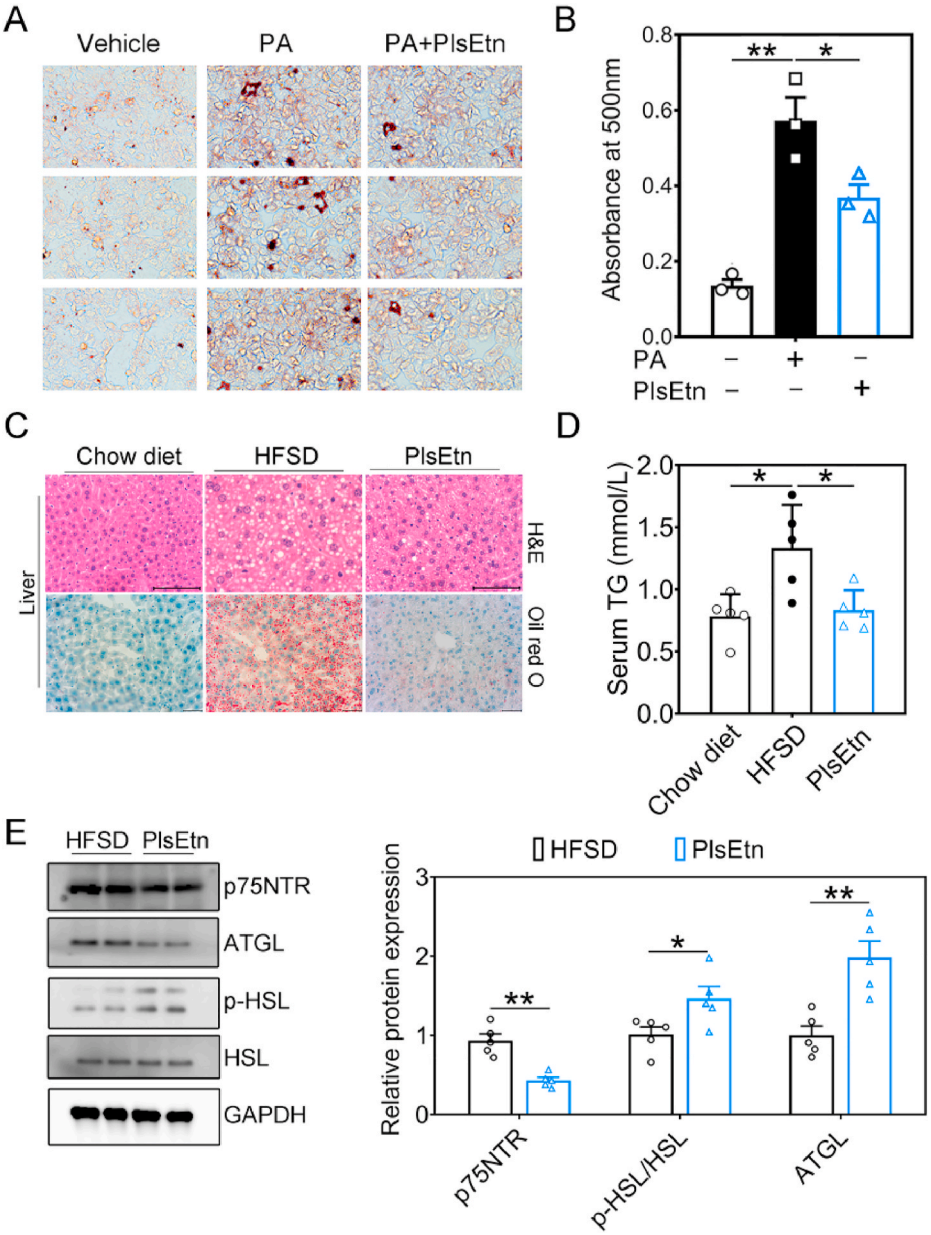

Fig. 3. PlsEtn supplementation ameliorates hepatic steatosis in HFSD-fed mice. (A and B) AML12 cells were exposed to 400 μM PA in the presence or absence of PlsEtn (200 μg ml^{-1}) for 48 h. Lipid droplets accumulation were determined by Oil-red O staining and quantified at 500 nm. (C) Photomicrographs depicting the liver from PlsEtn treated and HFSD-fed mice (n = 5 mice/group) stained for H&E and Oil red O. (D) Serum triglyceride levels in PlsEtn-treated APP/PS1 mice measured by lipids quantification. (E and F) Representative Western blot indicating the protein expression of p75NTR and lipolysis related genes in the liver of HFSD-fed mice (n = 5 mice/group). Statistical significance was determined by Student's *t*-test, *p < 0.05, **p < 0.01 vs HFSD-feed group; $^{\#}p < 0.05$, $^{\#\#}p < 0.01$ vs Chow diet group. (For interpretation of the references to colour in this figure legend, the reader is referred to the Web version of this article.)

from APP/PS1 mice, as shown by Oil Red O and H&E staining (Suppl. Fig. 3A–B). Similarly, significantly reduced hepatic triglyceride levels occurred in PlsEtn-treated APP/PS1 mice, as shown by lipids quantification (Suppl. Fig. 3C). In agreement with these findings, PlsEtn-treated mice had significantly reduced hepatic lipid accumulation after three months of HFSD challenge, which was corroborated by serum triglyceride levels and pathological results for the liver tissues from the mice in the various groups following Hematoxylin and Eosin (H&E) and Oil Red O staining (Fig. 3C–D). We further investigated whether PlsEtn treatment induces lipolysis and inhibits p75NTR in HFSD-fed mice. We observed decreased protein levels of p75NTR as well as increased ATGL protein expression and phosphorylation of HSL, which suggest higher

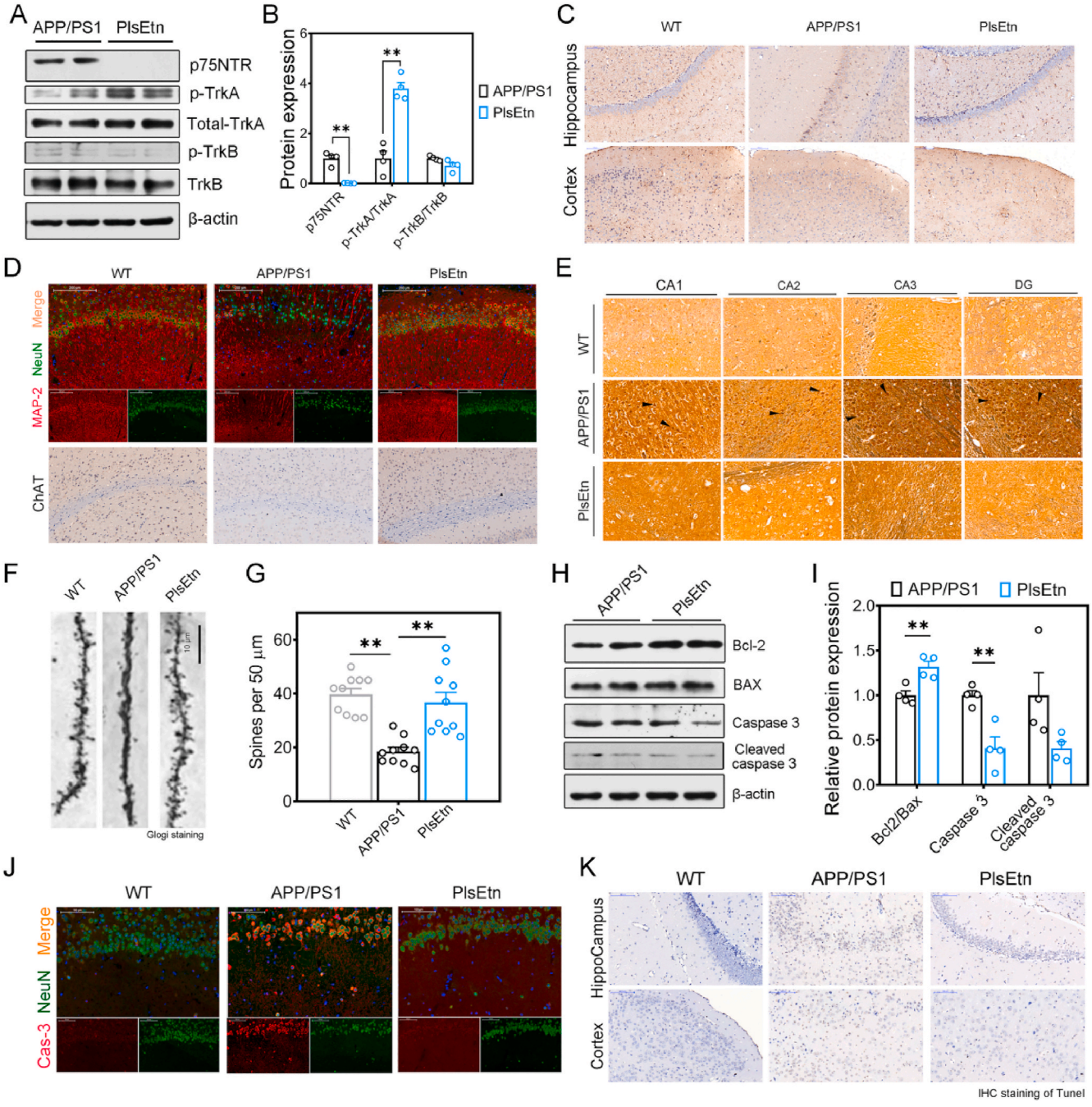

Fig. 4. PlsEtn treatment restores TrkA/p75NTR signaling, ameliorates neurodegeneration and neural death in APP/PS1 mice. (A and B) Representative Western blot indicating the expression of neurotrophins and their receptors in the hippocampus of APP/PS1 mice (n = 6 mice/group). (C) Photomicrographs depicting the hippocampus from APP/PS1 mice (n = 6 mice/group) stained for NGF. Scale bar, 200 μm. (D) Photomicrographs depicting the hippocampus from APP/PS1 mice (n = 6 mice/group) stained for MAP-2 (Red), NeuN (Green), and ChAT. Scale bar, 50 μm. (E) NFTs in APP/PS1 mice were reduced with the treatment of PlsEtn, as judged by a Bielschowsky silver staining method for detecting neurofibrillary tangles. Scale bar, 100 μm. (F and G) Dendritic spine and its density was conducted by Golgi staining measured then (n = 9 sections from 3 mice in each group). (H and I) Representative Western blot indicating the expression of apoptosis related markers in the hippocampus of APP/PS1 mice (n = 6 mice/group). (J) Photomicrographs depicting the hippocampus from APP/PS1 mice (n = 6 mice/group) stained for Cas3 (Red) and NeuN (Green). Scale bar, 50 μm. (K) Photomicrographs depicting the hippocampus from APP/PS1 mice (n = 6 mice/group) stained for TUNEL. Scale bar, 200 μm. Statistical significance was determined by Student's *t*-test, *p < 0.05, **p < 0.01 vs APP/PS1 mice; $^{\#}$p < 0.05, $^{\#\#}$p < 0.01 vs WT mice. (For interpretation of the references to colour in this figure legend, the reader is referred to the Web version of this article.)

lipolysis was induce by PlsEtn (Fig. 3E and F). Additionally, in HFSD-fed mice, glucose tolerance was markedly improved, with a reduction in body weight under PlsEtn (Suppl. Fig. 4A and B). PlsEtn attenuated insulin levels, and the level of fasting blood glucose was significantly reduced in these mice (Suppl. Fig. 4C and D). Consistent with these results, serum total cholesterol (TC) levels were significantly reduced by administration of PlsEtn (Suppl. Fig. 4E), while PlsEtn treatment has no effect on NEFA levels (Suppl. Fig. 4F). Collectively, the above results demonstrate that PlsEtn promotes lipolysis to improve lipid accumulation in liver via p75NTR inhibition in APP/PS1 mice and HFSD-fed mice.

3.4. Dietary PlsEtn restores TrkA/p75NTR imbalance and attenuates neurodegeneration and neuronal death in AD mice

Next, we set out to study whether p75NTR inhibition was involved in the role of plasmalogens on cognitive impairment. The p75NTR is not exclusively expressed by hepatocytes but also by neurons, playing a role for neurotrophin signaling in the neuronal function. Several lines of evidence indicate that dysregulated p75NTR lead to degeneration of basal forebrain cholinergic neurons (BFCN) and cognitive impairment in AD [26,30]. We supplemented APP/PS1 mice with PlsEtn to determine if plasmalogen contributed to p75NTR inhibition and attenuation of neurodegeneration. To assess whether tropomyosin-receptor kinase A (TrkA) receptor/p75NTR signaling were altered in the hippocampus of APP/PS1 mice treated by PlsEtn, we tested the neurotrophic factors levels and protein expressions of their receptors. Immunoblotting analysis revealed that phosphorylated TrkA were markedly activated after the treatment with PlsEtn, while p75NTR, another NGF receptor, were inhibited (Fig. 4A–B). In addition, we found that APP/PS1 mice exhibited a lower NGF expression, while supplementation of PlsEtn enhanced NGF expression as assessed by IHC staining compared with APP/PS1 mice (Fig. 4C). However, no significant changes in both of phospho-TrkB and total TrkB protein levels were found in the hippocampus of PlsEtn-fed mice (Fig. 4A–B).

TrkA/p75NTR imbalance could induce neurodegeneration and death [31], which are much studied features of AD pathology. To determine whether PlsEtn impact the AD-like neurodegeneration in APP/PS1 mice, hippocampus sections were used for anti-MAP-2 and anti-NeuN immunofluorescence. As indicated by staining for the mature neuronal markers, neuronal nuclei (NeuN), and the marker of neuronal differentiation, microtubule associated protein 2 (MAP-2), we observed lower labeling for NeuN and MAP-2 in the hippocampus of APP/PS1 mice compared with WT mice, while PlsEtn treatment increased immunoreactivity to neuronal marker NeuN and MAP-2 (Fig. 4D). Besides, PlsEtn increases the number of ChAT (Choline O-Acetyltransferase)-positive cells in APP/PS1 mice, which demonstrated that ChAT-positive neurons were restored by PlsEtn (Fig. 4D). AD is also pathologically characterized by the accumulation of neurofibrillary tangles (NFTs), which associated with tau pathology [32]. We found that NFTs appeared obviously in APP/PS1 mice but not in WT mice and APP/PS1 mice with the treatment of PlsEtn, as judged by a Bielschowsky silver staining method for detecting neurofibrillary tangles (Fig. 4E). As basic functional units of neuronal integration, dendritic spines are altered in number and shape before eventual neuronal death is observed in AD individual exhibiting cognitive impairments. Indeed, Golgi staining results (Fig. 4F–G) showed that the APP/PS1 mice exhibited significantly fewer dendritic branches and lower spine density in the hippocampal CA1 neurons than the WT mice. By contrast, PlsEtn-treated mice showed the increase in dendritic branches and spine density (Fig. 4F–G). p75NTR has been previously demonstrated to mediate neuronal apoptosis and is essential for sympathetic neuron death. In this study, the ratio of Bcl2/Bax was increased after PlsEtn treatment and the expression levels of caspase 3 were reduced after PlsEtn treatment, compared with the mice in APP/PS1 group (Fig. 4H–I), indicating that the PlsEtn treatment can suppressed the neuronal apoptosis in the hippocampus of AD mice. Consistent with the results, the fractional areas stained for NeuN- and Casp3 (caspase 3)-positive axons in the hippocampus were increased in PlsEtn-treated groups (Fig. 4J), when compared with APP/PS1 mice. In the TUNEL staining (Fig. 4K), the number of TUNEL positive cells was reduced after PlsEtn treatment.

3.5. Dietary PlsEtn ameliorates cognitive impairment in APP/PS1 mice

Lastly, to determine the effect of PlsEtn on spatial learning and memory, mice were tested at the end of the study, after 16 weeks of diet using the morris water maze test and radial 8-arm maze test. These mice showed different performances during the hidden platform tests (Fig. 5A). On first three day, there was no significant difference in the escape latency among all groups (Fig. 5A). However, the escape latency progressively decreased over the 5 days of training for WT mice, while APP/PS1 mice exhibited higher escape latency and impaired learning ability, compared to WT mice (Fig. 5A). At day 5, swimming paths of WT mice were highly concentrated in the target quadrant, whereas APP/PS1 mice frequently swam randomly in each quadrant without any purpose (Fig. 5B). In contrast, PlsEtn treatment increased the percentage of time spent in the target quadrant, and platform area crossings numbers (Fig. 5B–D). Compared with APP/PS1 mice, the mice receiving PlsEtn diet manifested a significant increase of the number of entries in the platform zone (Fig. 5C). Besides, there was no significant difference in the swimming speed among all groups (Fig. 5E), suggesting that their different performances during the hidden platform tests was unrelated to motor ability. Finally, the assessment of search strategy in the acquisition phase of the water maze test was performed. We observed that WT mice and the mice treated with PlsEtn showed preference for a spatial strategy, whereas APP/PS1 mice preferred to search for the platform by a repeated loop strategy (Fig. 5F–G). To investigate the effect of PlsEtn on spatial memory processing, all mice were trained during 6 days and the reference and working memory performance in each group were measured. Consistent with the result of morris water maze (MWM) test, the reference and working memory acquisition were increased in APP/PS1 mice, suggesting impaired spatial memory formation. By contrast, PlsEtn treatment showed improved reference and working memory acquisition (Suppl. Fig. 5A–B).

3.6. PlsEtn supplementation reduces Aβ and tau pathology in APP/PS1 mice

Studies have shown both of the accumulation of Aβ plaques and tau tangles pathologies in the brain are key features of AD [33,34]. IHC and IF staining of Aβ indicated that PlsEtn treatment reduced the Aβ-positive plaques in the cortex and hippocampus compared to those of untreated APP/PS1 mice (Fig. 5H–I). Elisa analysis confirmed a reduction of soluble and insoluble Aβ1-40 and Aβ1-42 levels after PlsEtn treatment (Fig. 5J–K). To understand the molecular underpinnings of these findings, we examined the expression of ADAM10 (α-secretase), BACE1 (β-secretase), and Nicastrin (γ-Secretase) proteins in hippocampus. We found that PlsEtn increased ADAM10 expression significantly, and reduced BACE1 expression in the hippocampus of APP/PS1 mice (Fig. 5L–M). Besides, PlsEtn has no effect on Nicastrin levels in APP/PS1 mice, which is different with the previous data on DHA-PlsEtn [35]. These results suggest that PlsEtn inhibits APP cleavage by the alteration of APP-processing, including α-secretase induction and β-secretase inhibition. PlsEtn treatment alleviated the expression of total Tau and phosphorylation of tau in hippocampus (Fig. 5N–O). Furthermore, PlsEtn treatment increased the ratio of *p*-GSK3β/GSK3β which leads to the inhibition of Tau phosphorylation. Histopathological analysis (Suppl. Fig. 6) confirmed a marked decrease in Tau protein expression of the hippocampus in PlsEtn-fed mice. Taken together, these observations provide evidence that PlsEtn reduces Aβ and regulate tau phosphorylation in APP/PS1 mice.

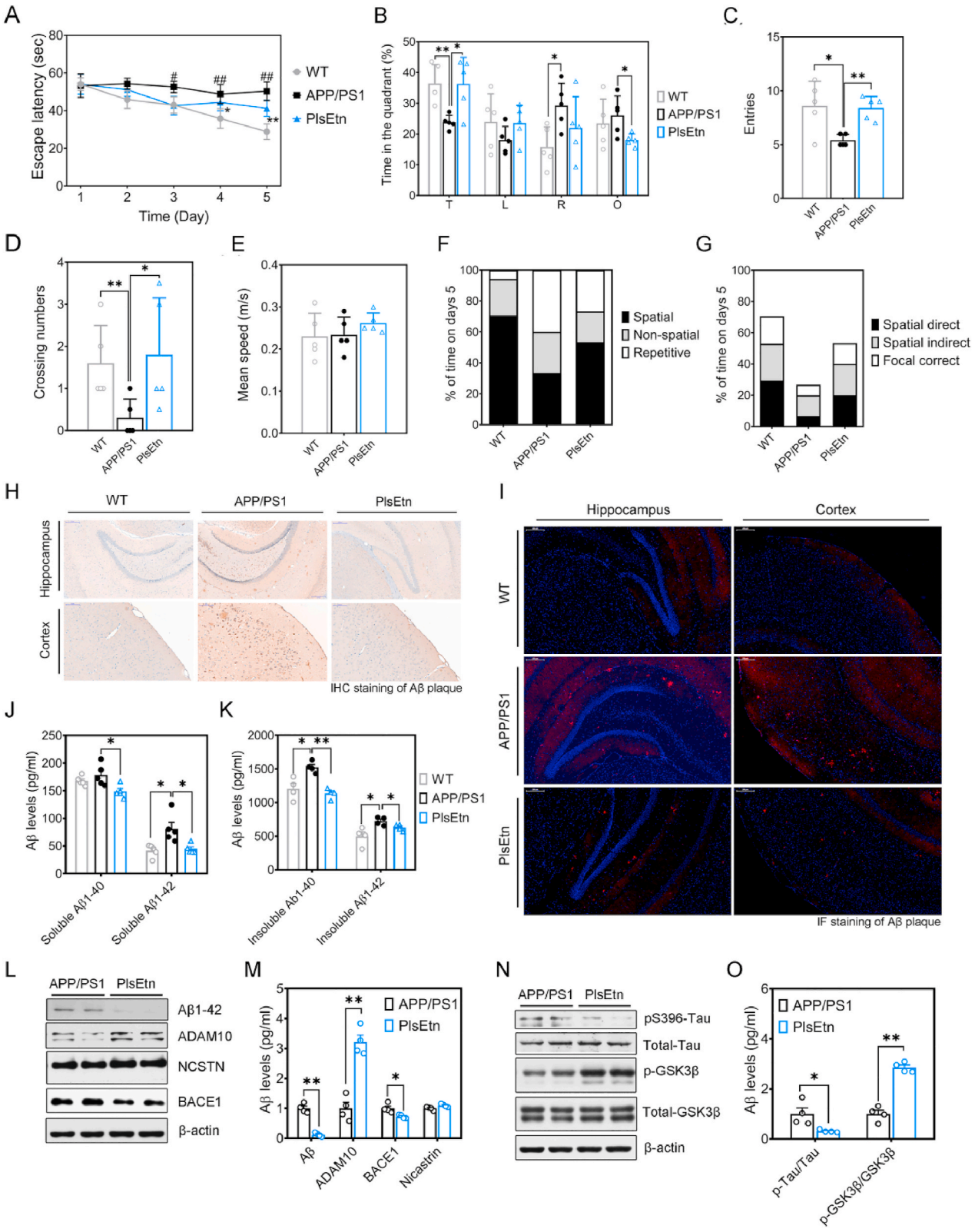

Fig. 5. PlsEtn supplementation ameliorates memory deficits, Aβ and Tau pathology. (A) Escape latency to the platform during the training trails in a Morris water maze (n = 5 mice/group). (B) Time spent in target quadrant in the MWM test at day 5. (C) Times crossing the target sites after retrieval of the platform at day 5. (D) Entries in target quadrant. (E) Average speed to find the platform. (F) Assessment of search strategy (spatial, non-spatial, repetitive) in the acquisition phase of the water maze test. (G) The percentage of time engaged in spatial search strategies during the 60-s trial was calculated, with search strategies combined into 3 groups based on functional similarity (Spatial Direct, Spatial Indirect, and Focal Correct strategies). (H and I) Photomicrographs of Aβ plaques within the hippocampus of APP/PS1 and PlsEtn-fed mice (n = 6 mice/group). Scale bar, 200 μm. (J and K) Quantitative analysis for the soluble and insoluble forms of Aβ1-40 and Aβ1-42 in hippocampus of APP/PS1 mice (n = 6 mice/group). (L and M) Representative Western blot of APP processing. (N and O) Representative Western blot of tau and p-Tau. Statistical significance was determined by Student's *t*-test, *$p < 0.05$, **$p < 0.01$ vs APP/PS1 mice; $^{\#}p < 0.05$, $^{\#\#}p < 0.01$ vs WT mice.

3.7. PlsEtn supplementation mitigates oxidative stress in APP/PS1 mice

Oxidative stress appear to be an early event in the etiology of AD, and plasmalogen has reported to suppress oxidative stress strongly in atherosclerosis and AD [16,35]. Hence, we further confirmed the effects of PlsEtn on oxidative stress in APP/PS1 mice. The results of the intracellular SOD (Superoxide Dismutase), NO (nitric oxide), and NOS (nitric oxide synthase) activity were shown in Table 1. It is known that SOD served as an important antioxidant enzyme in mitochondria against oxidative stress. APP/PS1 mice exhibited lower SOD activity than WT mice, whereas supplementation with PlsEtn significantly increased intracellular SOD activity of APP/PS1 mice. In addition, NO is a free radical with multiple functions in the mechanisms of Alzheimer's disease, and its main source in the brain is NOS enzymatic reaction. As expect, NOS activity were increased significantly in APP/PS1 mice, and resulted in increased NO level. Dietary PlsEtn led to a decline in the functions of both NO levels and NOS activity.

4. Discussion

Thus far, great efforts have been made to demonstrate the critical role of plasmalogen on the pathogenesis of AD and other metabolic diseases. For example, plasmalogen have been found to be associated with obesity, type 2 diabetes, atherosclerosis and Alzheimer's disease [3,36–38]. Furthermore, chronic exposure to diabetic environment with high-fat or high-glucose diet can cause hyperglycemia, the main characteristics of insulin resistance and diabetes, may resulting in a deterioration of cognitive function and hastening the incidence of AD due to the metabolic dysfunction [39]. The potential relationship between conditions such as diabetes and Alzheimer's diseases has been highlighted, and both of metabolic diseases and Alzheimer's disease are affected by lipid imbalances. Consistently, we observed that lipid droplet accumulation in the liver and brain of AD mice (Fig. 3) and represent lipid imbalance in AD, whereas PlsEtn treatment rescue the abnormal lipid accumulation as well as cognitive deficit. In this study, we tried to find its underlying mechanisms and have demonstrated p75NTR act as one of the potential mechanisms that underlie the benefits of PlsEtn on both of cognitive impairment and lipid accumulation in AD.

In a recent study, Mitchel Kling et al. reported that the liver could contribute to Alzheimer's risk by failing to supply PlsEtn to the brain [10]. As expected, we have demonstrated a reduction of PlsEtn levels and its de novo synthesis pathway impairment (reduced the mRNA expression of a rate-limiting enzyme, *Apgs* and *Gnpat*) occurred in both of brain and liver in APP/PS1 and HFD-fed mice. The possible mechanisms with regards to the decrease of PlsEtn in AD have been suggested including peroxisome dysfunction, and inflammatory responses. Indeed, peroxisome dysfunction events occurred in the liver and hippocampus of APP/PS1 mice, which may be required for PlsEtn reduction. Similar with our results, increased Aβ and ROS reduced the levels of PlsEtn due to the dysfunction of peroxisomes [3]. Besides, earlier studies have reported associations of plasmalogens with type 2 diabetes. In this regard, it has been reported that peroxisome deficiency induce fatty liver, cholestasis, and eventually cirrhosis [40]. In *C. elegans*, peroxisomal protein PEX5 mediates stimulated lipolysis [41], whereas lacking of PEX19 increased lipolysis and accumulation of free fatty acids are also present in human fibroblasts [42]. Thus, peroxisomes appears to make contact with the regulation of energy homeostasis and lipolysis, but the role of the PlsEtn synthesized in the peroxisomes on lipid homeostasis is largely unknown.

In another recent study, Lodhi et al. reported that adipose-specific knockout of the peroxisomal biogenesis factor PEX16 (PEX16-AKO) and knockdown of GNPAT in mice resulted in a reduction of plasmalogens and increased body weight, while dietary supplementation with alkylglycerols rescued thermogenesis in PEX16-AKO mice [38]. Their results suggests that peroxisomes/PlsEtn is a novel treatment option for obesity. Thus, we investigated how defective PlsEtn synthesis disrupts lipid accumulation in the AD and T2D liver and tested whether this could be reversed by the PlsEtn diet. To this end, we knocked down expression of GNPAT, the enzyme responsible for the first step in plasmalogen production, and observed that hepatic GNPAT knockdown induces hepatic steatosis and lipid accumulation in PA-treated AML12 cells, one of the symptoms of T2D and obesity. Consistently, inhibition of plasmalogen synthesis aggravates hepatic lipid accumulation in EtOH-treated AML12 cells. Notably, the effect of shGNPAT on aggravated lipid accumulation is due to inhibition of lipolysis in PA-treated AML12 cells. Interestingly, we observed that p75NTR expression increased in AML12 cells treated by shGNPAT as well as liver under pathological conditions in either APP/PS1 or HFD-fed mice, implying that p75NTR activation induced by PlsEtn deficiency was most likely correlated with the development of hepatic steatosis and lipid accumulation. Knockdown of p75NTR improve hepatic steatosis due to the regulation of lipolysis in PA-treated AML12 cells. Furthermore, we explored the possibility that restoration of plasmalogen levels by PlsEtn isolated from sea cucumber could relieve hepatic lipid accumulation and impaired lipolysis. From the results, PlsEtn treatment decreased p75NTR expression, improved hepatic lipid accumulation and activated lipolysis in HFSD-fed mice and APP/PS1 mice, suggesting that restoration of plasmalogens rescues lipid accumulation and lipolysis through p75NTR inhibition. Therefore, we highlight that p75NTR-mediated lipolysis is involved in the benefits of PlsEtn on hepatic lipid accumulation. Current findings indicate that p75NTR inhibition is involved in the positive role of PlsEtn on cognitive impairment and lipid accumulation. The plasmalogen levels in liver and hippocampus decreased due to the impairment of PlsEtn synthesis pathway and dysfunction of peroxisomes where plasmalogens are synthesized. Impairment of PlsEtn synthesis pathway, induced by GNPAT knockdown, resulted in abnormal hepatic lipid accumulation and inhibition of lipolysis via p75NTR activation in hepatocytes. In contrast, PlsEtn circumvents the issues of lipid accumulation in APP/PS1 and HFSD-fed mice liver by lipolysis activation regulated by p75NTR.

The p75NTR is not exclusively expressed by hepatocytes but also by cholinergic neurons in the basal forebrain, playing a role for neurotrophin signaling in the neuronal function. In our studies, we observed that both of liver and hippocampus exhibited increased p75NTR expression in APP/PS1 mice. Recent studies suggest that dysregulated p75NTR signaling lead to BFCN degeneration that is associated with cognitive impairment in AD [23]. Based all above data, we proposed a hypothesis that PlsEtn addition may improve neurodegenerative diseases via p75NTR inhibition. Of note, in sea cucumbers, plasmalogens with EPA in sn-2 is the main form of PlsEtn and enriched, which made sea cucumber as a good sources for PlsEtn. We investigated whether PlsEtn isolated from sea cucumber stimulate neurotrophin signaling in APP/PS1 mice. This notion is supported by the finding that treatment of PlsEtn led to activated TrkA signaling in hippocampus while reducing p75NTR activation, and elevated NGF levels in a APP/PS1 mouse model. In AD, p75NTR is able to mediate neuronal apoptosis and is involved in the pathogenesis of almost all hallmarks [23,43]. Indeed, we demonstrated PlsEtn treatment protected neurons against apoptotic cell death in APP/PS1 mice. In addition, TrkA/p75NTR has been shown to be the key mediators to determine the degree of synaptic plasticity and

Table 1
PlsEtn treatment mitigates oxidative stress.

Group	WT	APP/PS1	PlsEtn
SOD (U/mg prot)	129.58 ± 18.51	91.47 ± 5.96[a]	121.61 ± 10.51[c]
NO (μmol/g prot)	2.87 ± 0.54	4.36 ± 0.97[a]	3.19 ± 0.34[d]
NOS (U/mg prot)	1.35 ± 0.24	1.72 ± 0.15[b]	1.32 ± 0.20[d]

[a] $p < 0.01$.
[b] $p < 0.05$, vs WT mice.
[c] $p < 0.01$.
[d] $p < 0.05$, vs APP/PS1 mice.

dendritic density [43]. Further studies were performed to explore the effect of PlsEtn on synaptic damage and neuronal loss. We observed that PlsEtn treatment increased NeuN- and MAP-2-immunopositive cells. In APP/PS1 mice, the brains were characterized by the degeneration of dendritic spines as well as reduced dendritic density, while dietary PlsEtn reverse the loss of dendritic spines, as indicated by Golgi staining to detect the pathological changes. These data suggest that PlsEtn rescues the hippocampal synaptic plasticity impairment.

We further comprehensively evaluated the effect of PlsEtn on the cognitive impairment in a APP/PS1 mouse model of Alzheimer's disease. Our previous data show PlsEtn ameliorate cognitive function of high fat feeding SAMP8 mice by reduce BACE1 levels [44]. Our results illustrate that a long-term treatment of PlsEtn produces significant benefits on AD-like pathology and associated cognitive deficits in APP/PS1 mice. Besides, our data demonstrate that PlsEtn treatment significantly decreased Aβ and Tau deposits in the hippocampus and cortex. Similarly, administration of DHA-Plasmalogen was reported to attenuate the accumulation of Aβ proteins in lipopolysaccharide-treated mice [45]. The non-amyloidogenic APP processing pathway involves cleavages by α-secretase, while Aβ is released from APP processing via β-secretase and γ-secretase [46]. Notably, α-secretase (ADAM10) was increased, while β-secretase (BACE1) level was reduced by PlsEtn treatment, which suggests PlsEtn inhibit APP processing and Aβ generation. Of note, PlsEtn treatment has no effect on γ-secretase level, whereas DHA-plasmalogen was reported to reduce γ-secretase activity to reduce Aβ production in SH-SY5Y cells [34]. In conclusion, PlsEtn from sea cucumber is an effective pharmacological tool to prevent AD by significantly restoring TrkA/p75NTR balance in the brain, attenuating neurodegeneration and neuronal death, oxidative stress, and rescuing learning and memory impairments in APP/PS1 mice after long-term treatment. Therefore, together, these data indicate that the role of PlsEtn on cognitive impairment and hepatic steatosis is at least partially dependent on p75NTR inhibition. These exciting possibilities should be examined in future investigations for clinical.

Declaration of competing interest

The authors declare that they have no known competing financial interests or personal relationships that could have appeared to influence the work reported in this paper.

Acknowledgments

We greatly appreciate the financial support for this study provided from Ocean University of China. This work was supported by National Key R&D Program of China (No. 2018YFC0311201).

Appendix A. Supplementary data

Supplementary data to this article can be found online at https://doi.org/10.1016/j.redox.2021.102002.

Author contribution

All authors included in this manuscript have contributed to at least one of ICMJE guidelines. Jie Xu: conceived and planned the study Changhu Xue: conceived and planned the study Jingfeng Wang: conceived and planned the study Yuming Wang: conceived and planned the study Yanjun Liu: performed the cell and mice experiments, wrote the manuscript Junyi Liu: performed the cell and mice experiments Tao Zhang: performed the cell and mice experiments Xiaoxu Wang: performed the cell and mice experiments, performed lipid Formal analysis Peixu Cong: performed the cell and mice experiments, performed lipid Formal analysis Rui Wang: performed lipid Formal analysis.

Data availability

The data that support the findings of this study are available from the author (Yanjun Liu) upon reasonable request.

References

[1] S. Paul, G.I. Lancaster, P.J. Meikle, Plasmalogens: a potential therapeutic target for neurodegenerative and cardiometabolic disease, Prog. Lipid Res. 74 (2019) 186–195.
[2] S. Wallner, G. Schmitz, Plasmalogens the neglected regulatory and scavenging lipid species, Chem. Phys. Lipids 164 (2011) 573–589.
[3] X.Q. Su, J. Wang, A.J. Sinclair, Plasmalogens and Alzheimer's disease: a review, Lipids Health Dis. 18 (2019) 100.
[4] S. Oma, S. Mawatari, K. Saito, C. Wakana, Y. Tsuboi, T. Yamada, T. Fujino, Changes in phospholipid composition of erythrocyte membrane in Alzheimer's disease, Dement Geriatr Cogn Dis Extra. 2 (2012) 298–303.
[5] J.M. Weir, G. Wong, C.K. Barlow, M.A. Greeve, A. Kowalczyk, L. Almasy, A. G. Comuzzie, M.C. Mahaney, J.B.M. Jowett, J. Shaw, J.E. Curran, J. Blangero, P. J. Meikle, Plasma lipid profiling in a large population-based cohort, J. Lipid Res. 54 (2013) 2898–2908.
[6] P. Puri, M.M. Wiest, O. Cheung, F. Mirshahi, C. Sargeant, H.K. Min, M.J. Contos, R. K. Sterling, M. Fuchs, H. Zhou, S.M. Watkins, A.J. Sanyal, The plasma lipidomic signature of nonalcoholic steatohepatitis, Hepatology 50 (2009) 1827–1838.
[7] A. André, P. Juanéda, J.L. Sébédio, J.M. Chardigny, Plasmalogen metabolism-related enzymes in rat brain during aging: influence of n-3 fatty acid intake, Biochimie 88 (2006) 103–111.
[8] J.E. Jang, H.S. Park, H.J. Yoo, I.J. Baek, J.E. Yoon, M.S. Ko, A.R. Kim, H.S. Kim, H. S. Park, S.E. Lee, S.W. Kim, S.J. Kim, J. Leem, Y.M. Kang, M.K. Jung, C.G. Pack, C. J. Kim, C.O. Sung, I.K. Lee, J.Y. Park, J.C. Fernández-Checa, E.H. Koh, K.U. Lee, Protective role of endogenous plasmalogens against hepatic steatosis and steatohepatitis in mice, Hepatology 66 (2017) 416–431.
[9] M.A. Kling, D.B. Goodenowe, V. Senanayake, S. MahmoudianDehkordi, R. Baillie, X. Han, A. Kueider-Paisley, R.F. Kaddurah-Daouk, F3-02-04: serum indices of ethanolamine plasmalogens and phosphatide metabolism in the combined adni-1/go/2 cohort: does the liver contribute to ad risk by failing to supply key lipids to the brain? Alzheimer's Dement. 14 (2018) 998–999.
[10] M.A. Kling, D.B. Goodenowe, J.B. Toledo, V. Senanayake, R.A. Baillie, J.E. Lucas, J. D. Tenenbaum, A. Motsinger-Reif, X. Han, R.F. Kaddurah-Daouk, P3-157: indices of plasmalogen biosynthesis in ADNI-1 baseline serum samples: association with progression to dementia in subjects with mild cognitive impairment, Alzheimer's Dement. 12 (2016) 879–880.
[11] W. Lieb, A.S. Beiser, R.S. Vasan, Z.S. Tan, R. Au, T.B. Harris, R. Roubenoff, S. Auerbach, C. DeCarli, P.A. Wolf, S. Seshadri, Association of plasma leptin levels with incident Alzheimer disease and MRI measures of brain aging, JAMA, J. Am. Med. Assoc. 302 (2009) 2565–2572.
[12] P.J. Meikle, G. Wong, C.K. Barlow, J.M. Weir, M.A. Greeve, G.L. MacIntosh, L. Almasy, A.G. Comuzzie, M.C. Mahaney, A. Kowalczyk, I. Haviv, N. Grantham, D. J. Magliano, J.B.M. Jowett, P. Zimmet, J.E. Curran, J. Blangero, J. Shaw, Plasma lipid profiling shows similar associations with prediabetes and type 2 diabetes, PLoS One 8 (2013), e74341.
[13] T. Katafuchi, M. Ifuku, S. Mawatari, M. Noda, K. Miake, M. Sugiyama, T. Fujino, Effects of plasmalogens on systemic lipopolysaccharide-induced glial activation and β-amyloid accumulation in adult mice, Ann. N. Y. Acad. Sci. 1262 (2012) 85–92.
[14] M. Ifuku, T. Katafuchi, S. Mawatari, M. Noda, K. Miake, M. Sugiyama, T. Fujino, Anti-inflammatory/anti-amyloidogenic effects of plasmalogens in lipopolysaccharide-induced neuroinflammation in adult mice, J. Neuroinflammation 9 (2012) 197.
[15] L. Ding, L.Y. Zhang, H.H. Shi, C.C. Wang, X.M. Jiang, C.H. Xue, T. Yanagita, T. T. Zhang, Y.M. Wang, Eicosapentaenoic acid-enriched phosphoethanolamine plasmalogens alleviated atherosclerosis by remodeling gut microbiota to regulate bile acid metabolism in LDLR$^{-/-}$ mice, J. Agric. Food Chem. 68 (2020) 5339–5348.
[16] H. Che, Q. Li, T. Zhang, L. Ding, L. Zhang, H. Shi, T. Yanagita, C. Xue, Y. Chang, Y. Wang, A comparative study of EPA-enriched ethanolamine plasmalogen and EPA-enriched phosphatidylethanolamine on Aβ42 induced cognitive deficiency in a rat model of Alzheimer's disease, Food Funct. 9 (2018) 3008–3017.
[17] M.S. Hossain, K. Mineno, T. Katafuchi, Neuronal orphan G-protein coupled receptor proteins mediate plasmalogens-induced activation of ERK and Akt signaling, PLoS One 11 (2016), e0150846.
[18] M.S. Hossain, M. Ifuku, S. Take, J. Kawamura, K. Miake, T. Katafuchi, Plasmalogens rescue neuronal cell death through an activation of AKT and ERK survival signaling, PLoS One 8 (2013), e83508.
[19] J.K. Tomoko Onodera, Eugene Futai, Eiichiro Kan, Naoki Abe, Takafumi Uchida, Yoshiyuki Kamio, Phosphatidylethanolamine plasmalogen enhances the inhibiting effect of phosphatidylethanolamine on γ-secretase activity, J. Biochem. 157 (2015) 301–309.
[20] T. Fujino, T. Yamada, T. Asada, Y. Tsuboi, C. Wakana, S. Mawatari, S. Kono, Efficacy and blood plasmalogen changes by oral administration of plasmalogen in patients with mild Alzheimer's disease and mild cognitive impairment: a multicenter, randomized, double-blind, placebo-controlled trial, EBioMedicine 17 (2017) 199–205.

[21] Y.J. Wang, F. Zeng, K. Saadipour, J.J. Lu, X.F. Zhou, p75NTR: a molecule with multiple functions in amyloid-beta metabolism and neurotoxicity, in: Handb. Neurotox., Springer, New York, 2014, pp. 1925–1944.
[22] D.E. Bredesen, S. Rabizadeh, p75NTR and apoptosis: Trk-dependent and Trk-independent effects, Trends Neurosci. 20 (1997) 287–291.
[23] N.B. Mañucat-Tan, L.L. Shen, L. Bobrovskaya, M. Al-hawwas, F.H. Zhou, Y. J. Wang, X.F. Zhou, Knockout of p75 neurotrophin receptor attenuates the hyperphosphorylation of Tau in pR5 mouse model, Aging (N Y) 11 (2019) 6762–6791.
[24] F. Zeng, J.J. Lu, X.F. Zhou, Y.J. Wang, Roles of p75NTR in the pathogenesis of Alzheimer's disease: a novel therapeutic target, Biochem. Pharmacol. (2011) 1500–1509.
[25] B. Baeza-Raja, B.D. Sachs, P. Li, F. Christian, E. Vagena, D. Davalos, N. Le Moan, J. K. Ryu, S.L. Sikorski, J.P. Chan, M. Scadeng, S.S. Taylor, M.D. Houslay, G.S. Baillie, A.R. Saltiel, J.M. Olefsky, K. Akassoglou, p75 neurotrophin receptor regulates energy balance in obesity, Cell Rep. 14 (2016) 255–268.
[26] Y. Abe, M. Honsho, R. Itoh, R. Kawaguchi, M. Fujitani, K. Fujiwara, M. Hirokane, T. Matsuzaki, K. Nakayama, R. Ohgi, T. Marutani, K.I. Nakayama, T. Yamashita, Y. Fujiki, Peroxisome biogenesis deficiency attenuates the BDNF-TrkB pathway-mediated development of the cerebellum, Life Sci. Alliance 1 (2018).
[27] C. Kilkenny, W. Browne, I.C. Cuthill, M. Emerson, D.G. Altman, Animal research: reporting in vivo experiments: the ARRIVE guidelines, Br. J. Pharmacol. 160 (2010) 1577–1579.
[28] L. Ding, L. Zhang, H. Shi, C. Xue, T. Yanagita, T. Zhang, Y. Wang, EPA-enriched ethanolamine plasmalogen alleviates atherosclerosis via mediating bile acids metabolism, J. Funct. Foods 66 (2020) 103824.
[29] M.J. Curtis, S. Alexander, G. Cirino, J.R. Docherty, C.H. George, M.A. Giembycz, D. Hoyer, P.A. Insel, A.A. Izzo, Y. Ji, D.J. MacEwan, C.G. Sobey, S.C. Stanford, M. M. Teixeira, S. Wonnacott, A. Ahluwalia, Experimental design and analysis and their reporting II: updated and simplified guidance for authors and peer reviewers, Br. J. Pharmacol. 175 (2018) 987–993.
[30] A.M. Fortress, M.H. Buhusi, K.L. Helke, A.C.E. Granholm, Cholinergic degeneration and alterations in the TrkA and p75NTR balance as a result of pro-NGF injection into aged rats, J. Aging Res. 2011 (2011) 460543.
[31] A. Kimura, K. Namekata, X. Guo, C. Harada, T. Harada, Neuroprotection, growth factors and BDNF-TRKB signalling in retinal degeneration, Int. J. Mol. Sci. 17 (2016).
[32] C. Andorfer, Y. Kress, M. Espinoza, R.D. Silva, K.L. Tucker, Y. Barde, K. Duff, P. Davies, Hyperphosphorylation and aggregation of tau in mice expressing normal human tau isoforms, J. Neurochem. 86 (3) (2003) 582–590.
[33] F. Bassil, H.J. Brown, S. Pattabhiraman, J.E. Iwasyk, C.M. Maghames, E. S. Meymand, T.O. Cox, D.M. Riddle, B. Zhang, J.Q. Trojanowski, V.M.Y. Lee, Amyloid-beta (Aβ) plaques promote seeding and spreading of alpha-synuclein and tau in a mouse model of Lewy body disorders with Aβ pathology, Neuron 105 (2020) 260–275.
[34] T.L. Rothhaar, S. Grösgen, V.J. Haupenthal, V.K. Burg, B. Hundsdörfer, J. Mett, M. Riemenschneider, H.S. Grimm, T. Hartmann, M.O.W. Grimm, Plasmalogens inhibit APP processing by directly affecting γ-secretase activity in Alzheimer's disease, Sci. World J. 2012 (2012).
[35] J. Lessig, B. Fuchs, Plasmalogens in biological systems: their role in oxidative processes in biological membranes, their contribution to pathological processes and aging and plasmalogen analysis, Curr. Med. Chem. 16 (2009) 2021–2041.
[36] D.B. Goodenowe, L.L. Cook, J. Liu, Y. Lu, D.A. Jayasinghe, P.W.K. Ahiahonu, D. Heath, Y. Yamazaki, J. Flax, K.F. Krenitsky, D.L. Sparks, A. Lerner, R. P. Friedland, T. Kudo, K. Kamino, T. Morihara, M. Takeda, P.L. Wood, Peripheral ethanolamine plasmalogen deficiency: a logical causative factor in Alzheimer's disease and dementia, J. Lipid Res. 48 (2007) 2485–2498.
[37] H. Park, A. He, M. Tan, J.M. Johnson, J.M. Dean, T.A. Pietka, Y. Chen, X. Zhang, F. F. Hsu, B. Razani, K. Funai, I.J. Lodhi, Peroxisome-derived lipids regulate adipose thermogenesis by mediating cold-induced mitochondrial fission, J. Clin. Invest. 129 (2019) 694–711.
[38] H.J. Lee, H.I. Seo, H.Y. Cha, Y.J. Yang, S.H. Kwon, S.J. Yang, Diabetes and Alzheimer's disease: mechanisms and nutritional aspects, Clin. Nutr. Res. 7 (2018) 229.
[39] M. Baes, P.P. Van Veldhoven, Mouse models for peroxisome biogenesis defects and β-oxidation enzyme deficiencies, Biochim. Biophys. Acta (BBA) - Mol. Basis Dis. 1822 (2012) 1489–1500.
[40] J. Kong, Y. Ji, Y.G. Jeon, J.S. Han, K.H. Han, J.H. Lee, G. Lee, H. Jang, S.S. Choe, M. Baes, J.B. Kim, Spatiotemporal contact between peroxisomes and lipid droplets regulates fasting-induced lipolysis via PEX5, Nat. Commun. 11 (2020).
[41] M.H. Bülow, C. Wingen, D. Senyilmaz, D. Gosejacob, M. Sociale, R. Bauer, H. Schulze, K. Sandhoff, A.A. Teleman, M. Hoch, J. Sellina, Unbalanced lipolysis results in lipotoxicity and mitochondrial damage in peroxisome-deficient Pex19 mutants, Mol. Biol. Cell 29 (2018) 396–407.
[42] L.F. Reichardt, Neurotrophin-regulated signalling pathways, Philos. Trans. R. Soc. B Biol. Sci. 361 (2006) 1545–1564.
[43] X.Q. Yao, S.S. Jiao, K. Saadipour, F. Zeng, Q.H. Wang, C. Zhu, L.L. Shen, G.H. Zeng, C.R. Liang, J. Wang, Y.H. Liu, H.Y. Hou, X. Xu, Y.P. Su, X.T. Fan, H.L. Xiao, L. F. Lue, Y.Q. Zeng, B. Giunta, J.H. Zhong, D.G. Walker, H.D. Zhou, J. Tan, X. F. Zhou, Y.J. Wang, P75NTR ectodomain is a physiological neuroprotective molecule against amyloid-beta toxicity in the brain of Alzheimer's disease, Mol. Psychiatr. 20 (2015) 1301–1310.
[44] H. Che, M. Zhou, T. Zhang, L. Zhang, L. Ding, T. Yanagita, J. Xu, C. Xue, Y. Wang, EPA enriched ethanolamine plasmalogens significantly improve cognition of Alzheimer's disease mouse model by suppressing β-amyloid generation, J. Funct. Foods 41 (2018) 9–18.
[45] T. Katafuchi, M. Ifuku, S. Mawatari, M. Noda, K. Miake, M. Sugiyama, T. Fujino, Effects of plasmalogens on systemic lipopolysaccharide-induced glial activation and β-amylold accumulation in adult mice, Ann. N. Y. Acad. Sci. 1262 (2012) 85–92.
[46] C. Haass, C. Kaether, G. Thinakaran, S. Sisodia, Trafficking and proteolytic processing of APP, Cold Spring Harb. Perspect. Med. 2 (2012) a006270.